Plasma Reflectometry Applied to Plume Density Measurements of Electric Propulsion Thrusters

IEPC-2009-041

Presented at the 31st International Electric Propulsion Conference,
University of Michigan • Ann Arbor, Michigan • USA
September 20 – 24, 2009

Sérgio Mota[1], David P. Resendes[2] and Luis Cupido[3]
Instituto de Plasmas e Fusão Nuclear / Instituto Superior Técnico (IPFN/IST)
Av. Rovisco Pais 1, Lisbon, 1049, Portugal

Abstract: A frequency modulated continuous wave (FMCW) plasma reflectometer, under development for plasma sheath profile determination of a planetary re-entry vehicle, is currently being tested at the large plasmatron facility of the von Kárman Institute in Belgium. The plasma generated by the plasmatron has many similarities with the plumes generated by Electric Propulsion (EP) thrusters. As such, plasma reflectometry could prove to be a useful diagnostic for EP thrusters. The reflectometer design and first plasma measurement results are presented.

Nomenclature

c	=	speed of light in vacuum
F	=	source frequency
F_{pe}	=	plasma electron frequency
F_s	=	sampling rate
f	=	frequency
f_b	=	beat frequency
m_e	=	mass of electron
N_{FFT}	=	spectral length
n_e	=	plasma electron density
q_e	=	electron charge
R	=	distance from antenna reference plane
V	=	control voltage
T	=	sweep interval (p. 5), temperature of component (p. 6)
Δr	=	spatial resolution
δt	=	plasma flow time
ε_0	=	permittivity of vacuum
τ	=	total propagation delay
τ_0	=	reference propagation delay
τ_p	=	propagation delay in plasma

[1] Researcher, IPFN/IST, smota@ist.utl.pt.
[2] Professor, IPFN/IST, resendes@ist.utl.pt.
[3] Professor, IPFN/IST and Univ. Aveiro, cupido@mail.ua.pt.

I. Introduction

Nonintrusive radio frequency diagnostics of plasma density and temperature are well recognized for their accuracy and convenience of measurement in a number of fields such as fusion research and plasma processing.[1-4] Interest has also increased recently in using microwave interferometric measurement techniques of plasma plumes generated by high energy electric propulsion (EP) thrusters.[5-10] Experimentally characterizing the interaction of a microwave signal with an EP thruster plume can provide a direct measure of line-integrated electron number density.[11-17] The method avoids the issues of probe heating and local plasma perturbations of *in situ* techniques in dense energetic plasmas. A few systems can generate spatial mapping in one plane, but it would be desirable to provide spatial mapping in two planes of the plasma. Present systems are limited when compensating for vacuum chamber effects such as chamber resonances or multipath since most use single frequencies and traditional phase detector circuits for the interferometric phase comparison.

Interferometry gives only a path integrated result from which the plasma profile properties may be inferred by various symmetry assumptions from the distortion to the probing electromagnetic wave (phase and amplitude). Reflectometry which relies on electromagnetic reflection from the critical plasma layer, on the other hand, provides detailed profile information along a line of sight and, from successive measurements, the volume distribution of plasma can be obtained. Re-entry plasma reflectometry has been developed as a horizontal precursor flight technology able to provide plasma flow-field information not possible with other instruments. Such information is crucial for vehicle design, aeroassist/aerobrake technology, and communications blackout control, particularly for newer generation, high speed re-entry scenarios. Such an instrument can also provide important scientific data if deployed on high speed planetary/lunar/cometary probes and sample return vehicles.

The Re-Entry Plasma Broadband Reflectometer (RPBR) breadboard, developed under ESA funding, is a swept Frequency Modulated Continuous Wave (FMCW) reflectometer. A data inversion slope method was shown to be the best option, providing detailed plasma density profile determination with a relatively simple, reliable technology implementation. Full profile determination can be made on a time scale of a few milliseconds, allowing for a large number of profile measurements along the trajectory, as much as one profile determination every few tens of meters along the flight path. Compact, high capacity flash memory allows for data storage for post-flight analysis. Testing of the RPBR is being performed in the plasmatron at the Von Karman Institute (VKI). While this plasma is deemed appropriate to simulate a re-entry plasma, there are significant differences. Under re-entry, the plasma is generated by shock heating and vehicle friction rather than by induction coils with oscillating currents. In the plasmatron, the plasma density is controlled by the power deposited in the neutral gas flow. As such, the re-entry plasma is expected to be steadier than the plasma produced by the plasmatron. However, background pressures and neutral gas flow velocity can be adjusted in the plasmatron to simulate those under re-entry conditions so that heat fluxes and vehicle surface temperatures may be similar. The specific characteristics of the VKI plasma naturally impacted reflectometer operating parameters. More importantly in the present context, the plasma generated by the plasmatron shares many characteristics with plasmas generated in a Hall Effect Thruster (HET).

In this article the relevant plasma characteristics for reflectometry of a plasmatron and an HET will be discussed. This will be followed by the major design considerations of the RPBR instrument. First plasma measurement results will then be presented. The article ends with the main conclusions of this technology development.

II. Plasma Characteristics

A plasmatron is a plasma wind tunnel using an Inductively Coupled Plasma (ICP) torch as plasma source. Its application to high enthalpy wind tunnel research is mainly due to the high purity and high energy density flow characteristics which are particularly interesting for aerothermodynamic studies. The torch in the VKI plasmatron is mounted on a 1.4 m diameter, 2.5 m long, water-cooled test chamber kept at sub-atmospheric pressure (between 5 and 175 mbar), and fitted with nine 500 mm diameter portholes that allow unrestricted optical access to the horizontally oriented plasma jet.[18]

Unsteadiness of the discharge is a complex problem due to the coupling between parameters. Two main sources of unsteadiness can be distinguished, namely, electrical effects and fluid dynamic effects. The electrical fluctuations, due to the time varying electromagnetic fields, represent a very high frequency ($1/f = 10^{-6}$ s) effect which averages over the characteristic time of the flow ($\delta t \sim 10^{-3}$ s). Some interactions exist, for instance, the modulation of the current after the rectifier, in the power generator, is reflected in the energy deposition in the plasma discharge. This phenomenon occurs on a time scale of the order of the flow time ($\delta t \sim 10^{-3}$ s), and can be reduced by adjusting the plasma setting. Two oscillation periods have been identified under normal operation; 1.66×10^{-3} s (600 Hz) and 8.33×10^{-4} s (1200 Hz, 2nd harmonic). In addition, the confined recirculation zone in the ICP torch induces vortex shedding and creates unsteadiness traveling in the plasma flow.

CFD simulations of the Plasmatron operation have been performed by VKI in support of measurements. For the reflectometer measurements, the plasma density distribution is of direct interest. A sample simulation appears in Fig. 1 below.[19] From this figure, it can be seen that on axis at the stagnation point 40 cm downstream from the plasma jet exit plane, i.e. at x=0.9 m, the predicted plasma density is of order 10^{20} m^{-3} (10^{14} cm^{-3}). The density decays along the axis from the exit plane, and, for a given axial position, decreases radially away from the axis. This behavior is significant for reflectometry which requires a monotonically increasing plasma profile. In propagating across an increasing density profile, an electromagnetic wave of fixed frequency travels up to the point where the wave frequency equals the local plasma frequency. At this point the wave is reflected. To map the full density profile at the 40 cm position would therefore require wave frequencies up to 100 GHz. The set of measurements reported here (cf. sec. IV) had wave frequencies varying between 12 and 18 GHz, or correspondingly, densities between 1.79×10^{18} m^{-3} (1.79×10^{12} cm^{-3}) and 4.02×10^{18} m^{-3} (4.02×10^{12} cm^{-3}).

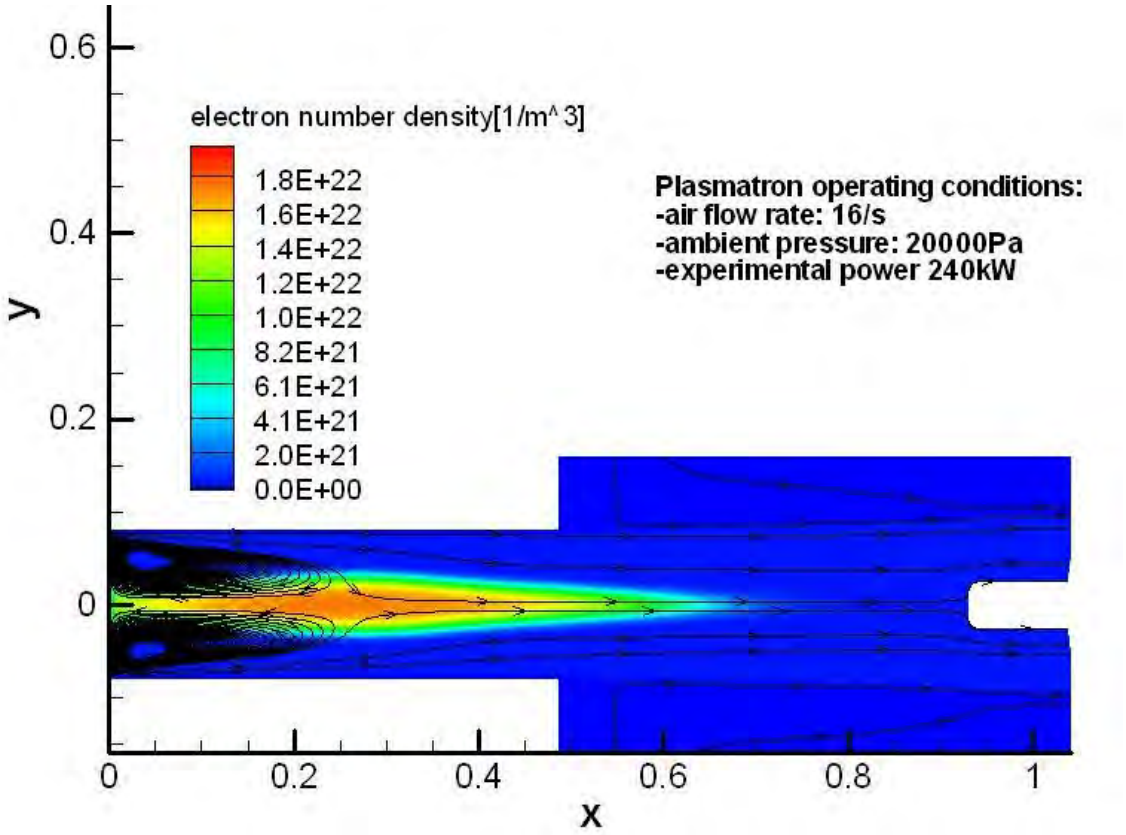

Figure 1. CFD simulation of the electron plasma density in the VKI plasmatron. X and y values are in meters.

From the above considerations, it is seen that obtaining viable profiles of the electron density in the Plasmatron places stringent requirements not only on the sweep interval of the reflectometer (which needs to be typically less than 10% of the smallest characteristic period of the plasma oscillation of 0.8 ms), but also on the receiver amplifier, which needs to compensate for a large variability of the received power. Fast sweeping and signal amplification received particular attention. All high frequency plasma oscillations are averaged over by the instrument. Additionally, the geometry of the VKI chamber places additional constraints on the reflectometer. In particular, the metallic nature of the plasmatron produces reflections which interfere with the desired signal. To remove these interferences, appropriate range gating must be implemented which is achieved through filtering.

By comparison, the plasma density in the far-field plume (>5cm downstream of the exit plane) of the BHT-200 thruster displays similar qualitative behavior as the VKI plasmatron, though absolute values differ, cf. Fig. 2.[20] For the BHT-200 thruster, a well-defined jet structure with a peak density near the thruster centerline is visible. The plasma density is high near the thruster centerline and decreases rapidly in both the axial and transverse directions as the plume expands. The peak density recorded by a triple probe was about 1.2×10^{18} m^{-3} (1.2×10^{12} cm^{-3}) while a Langmuir probe peaked at approximately 7.0×10^{17} m^{-3} (7.0×10^{11} cm^{-3}).

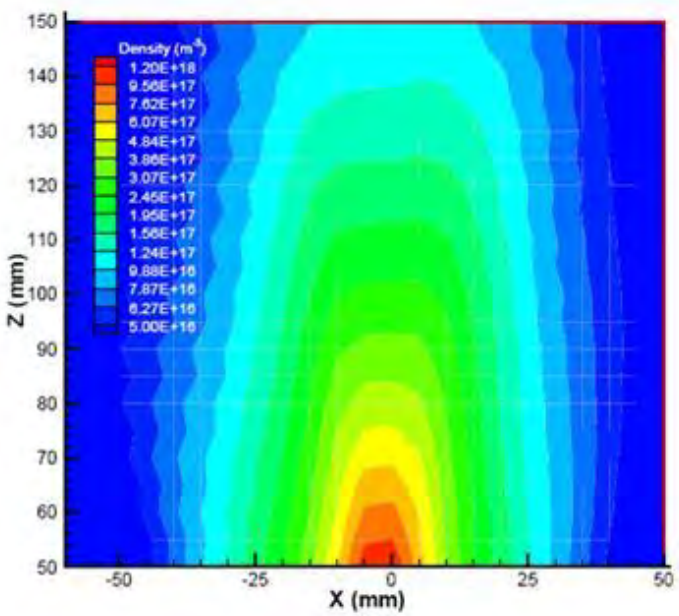

Figure 2. Plasma density in the far-field plume of the BHT-200 thruster measured using a triple probe

The oscillation spectrum in HET thrusters ranges from the ion cyclotron frequency in the kilohertz range up to the electron plasma frequency in the gigahertz range. Between these limits, several well-defined frequency bands can be identified. Low-frequency current oscillations of about 20 kHz, often referred to as "breathing oscillations",[21] may be explained as a result of displacement of the ionization front inside the thruster channel. Such oscillations are of primary importance for thruster performance and lifetime. Oscillations in the frequency range 100–500 kHz are often called "transit-time" oscillations because their frequency scales with inverse ion residence time in thruster channel.[22-23] It is thought they manifest themselves as plasma density fluctuations propagating along the channel. Lastly, oscillations with frequencies in the range of a few megahertz are associated with electrostatic waves propagating azimuthally.[22-25] In particular, these high-frequency oscillations are expected to be responsible for turbulent electron transport across the magnetic barrier.[26] All of these oscillations are effectively averaged over with the reflectometer described in this work.

III. Reflectometry Design

An incident electromagnetic wave of frequency F will propagate freely in a non-magnetized plasma only in such regions for which $F > F_{pe}$, where F_{pe} is the *plasma electron frequency* which depends on the electron density n_e and is given in SI units by

$$F_{pe} = \frac{1}{2\pi}\left(\frac{q_e^2 n_e}{\epsilon_0 m_e}\right)^{1/2}. \tag{1}$$

In regions where the condition $F > F_{pe}$ is not verified, the incident wave will be progressively reflected as it penetrates the plasma. Under appropriate conditions, the reflection occurs over a small volume very near the surface where the plasma electron frequency equals the incident wave frequency, i.e. where $F_{pe} = F$. This surface then acts as a perfect reflecting layer, which position depends on the particular frequency F that is selected, cf. Fig 3. Thus, a scan of the plasma volume can be implemented in effect simply by sweeping the frequency of the probing wave. In such a swept frequency system, the reflected signal that is picked up by the receiver exhibits a frequency offset with respect to the source signal resulting from the propagation not only inside the plasma, but also in the intervening waveguides, coaxial cables and circuit components. This frequency offset, f_b, is estimated by spectral methods and then translated to total propagation delay, $\tau = \tau_0 + \tau_p$

$$\tau = \left|\frac{dF}{dt}\right|^{-1} f_b. \tag{2}$$

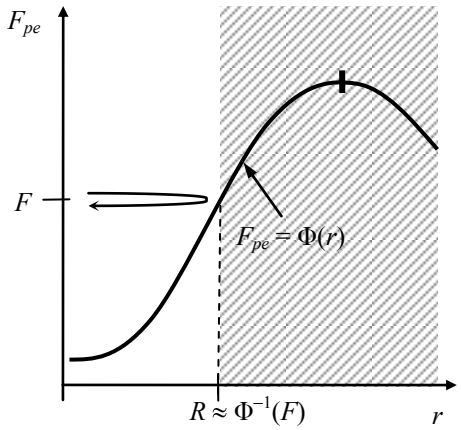

Figure 3. Reflectometry principle

Equation (2) is used under the assumption that the oscillations of the plasma layers are small and result in negligible Doppler shifts. After the known contribution τ_0 of the intervening waveguides, coaxial cables and circuit components is discounted from τ, an estimate of the group delay in plasma $\tau_p(F)$ results which is used in the determination of the plasma electron density profile through an Abel inversion

$$R(F_{pe}) \equiv \frac{c}{\pi}\int_0^{F_{pe}} \frac{\tau_p(F)}{\sqrt{F_{pe}^2 - F^2}}\, dF. \tag{3}$$

The reflectometer frequency F is swept in the range 2 GHz to 18 GHz. This range is sufficient for probing electron densities n_e in the range 4.96×10^{16} m^{-3} to 4.02×10^{18} m^{-3} (4.96×10^{10} cm^{-3} to 4.02×10^{12} cm^{-3}). The sweep interval T is currently less than 100 μs and signals may be acquired continuously for up to 10 milliseconds at a time, or 100 sweeps. Thus, the system is capable of following plasma fluctuations from 5 kHz down to 50 Hz. The spatial resolution Δr that can be obtained with this equipment, using an acquisition system working at a sampling rate F_s of 16 million samples per second and a spectral length N_{FFT} of 1024 samples in processing, is less than 1.5 cm. Table 1 summarizes the important parameter values.

Table 1. Performance Parameters

Frequency range, F	2 GHz to 18 GHz
Electron density range, n_e	4.96×10^{16} m^{-3} to 4.02×10^{18} m^{-3}
Sweep interval, T	< 100 μs
Sampling rate, F_s	16 MS/s
Sampling resolution	12 bits
Storage	2 MB
Measurement length	100 sweeps
Plasma fluctuation	50 Hz to 5 kHz
Spectral length, N_{FFT}	1024 samples
Spatial resolution, Δr	< 1.5 cm

The fact that the start frequency is not zero, implies that in Eq. (3) additional data has to be included in the form of an estimate of $\tau_p(F)$ for the range of frequencies from zero up to the start frequency.

The functional model of the reflectometer is composed of several functional blocks or modules, as presented in Fig. 4. The controller device is at the heart of the instrument. It serves different purposes: 1) generate control data that is translated to a particular waveform to drive the oscillators; 2) synchronize source signal with acquisition; and 3) retrieve data from acquisition buffer and store it on disk. From the control data, the digital/analog converter (DAC) or ramp generator outputs a particular waveform, $V(t)$, usually a triangular waveform with a slightly modulated slope to compensate for nonlinearities in the oscillator"s characteristic functions. By changing the control data, the controller device can alter the waveform at any time during operation of the instrument. The voltage controlled oscillator outputs a signal of modulated frequency F which is a known function of the control voltage V and of temperature T. The transmit/receive (T/R) module transmits the source signal to the antenna and collects the reflected signal from the plasma. The outputs of the T/R module are a reference signal of frequency F and a reflected signal of frequency F-f_b. Single side band mixing of these signals within the detector will result in a „beat signal" of frequency f_b. Knowledge of frequency f_b is sufficient for obtaining the total propagation delay τ. The information required for the data processing stage is obtained by the analog/digital converter (ADC) and includes the samples s_i of the plasma signal, the samples (V_i,T_i) of the control voltage and temperature in the signal generator module and the time tag t_i obtained from the CPU clock, or externally.

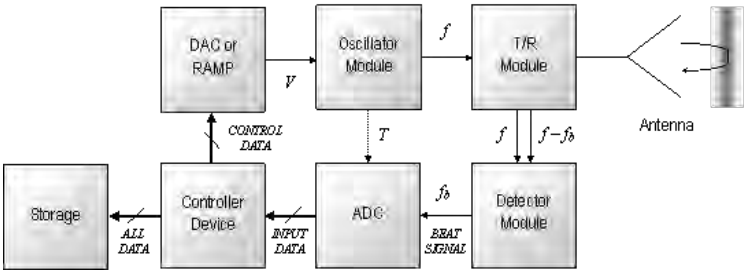

Figure 4. Functional model

The system is designed to work not only as a reflectometer in a monostatic configuration, i.e. with a single antenna doing double duty as transmitter and receiver; but also as a reflectometer in bistatic configuration, in which two antennas are employed, one as transmitter and the other as receiver; and finally, as an interferometer for measurement of transmissivity in the plasma. The two antennas are connected to the body of the reflectometer by microwave cables of approximately 1.5 m in length each. The schematic in Fig. 5 shows a typical arrangement of the various microwave encapsulated components, control and acquisition units and signal conditioning electronics that make up the diagnostic instrument. Access to the plasma channel is usually accomplished through a vacuum window that is transparent to microwaves in the frequencies of interest, but direct access is also an option on some test facilities.

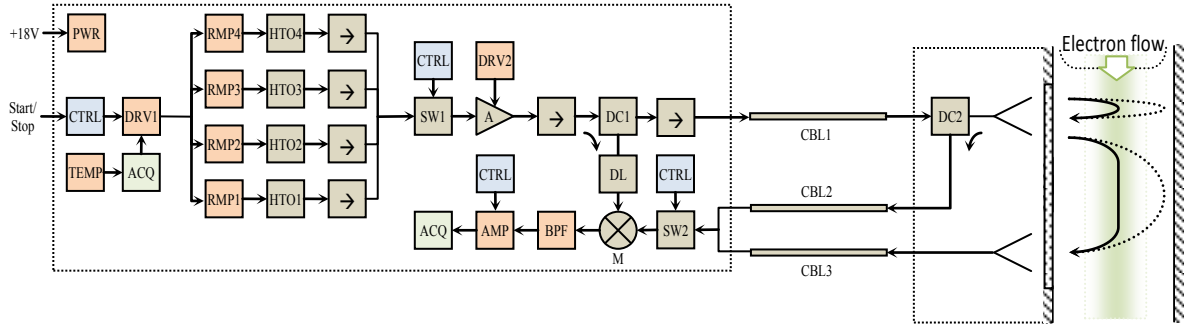

Figure key: PWR power supply, CTRL controller unit, TEMP temperature sensor, ACQ acquisition unit, DRV driver circuit, RMP ramp generator, HTO microwave source, → microwave isolator, SW solid state switch, A power amplifier, DC directional coupler, DL delay line, CBL coaxial cable, < rectangular horn antennas, M downconversion mixer, BPF band pass filter, AMP signal amplifier.

Figure 5. Circuit schematic

IV. First Results

Initial tests were conducted in April and August 2009 at the von Kárman Institute for Fluid Dynamics in Brussels, Belgium, on the Plasmatron facility (cf. Fig. 6 and section II). The main objectives were: 1) to observe the reflection of microwaves in a real plasma; 2) measure the level of reflected power and ensure it met the requirements for detection; 3) test the operation of the diagnostic instrument and of the signal conditioning electronics; 4) obtain preliminary data for testing the data processing procedures, spectral analysis and Abel inversion; and 5) diagnose hardware problems in a real experimental setting.

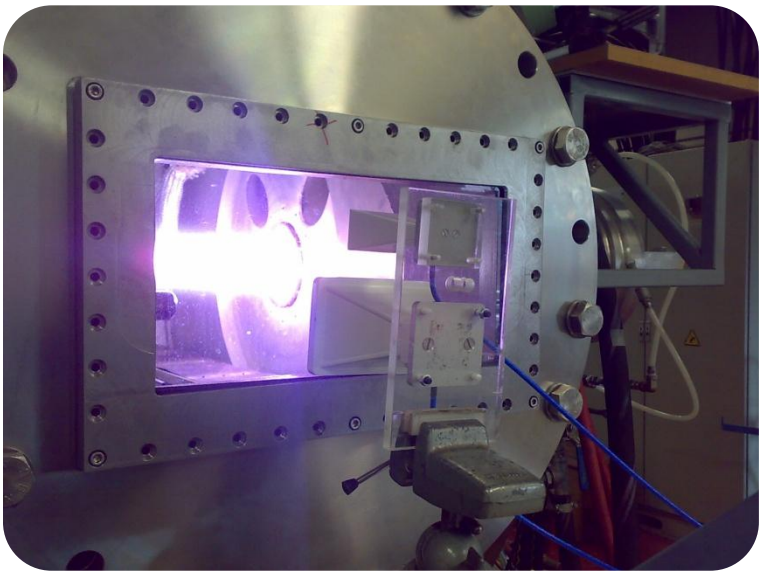

Figure 6. Antenna setup showing Plasmatron in operation

The diagnostic was setup in a bistatic configuration, with a larger rectangular horn antenna as the emitter and a smaller one in the receiving end, mounted parallel to one another and flushed with the external surface of the Plasmatron observation window, centered vertically, and aligned perpendicularly to the axis of the plasma jet. The plasma was scanned in the frequency range of 12 GHz to 18 GHz, which required the use of only one of the four microwave sources available and allowed a smaller prototype of the instrument to be used in the experiments, cf. Fig. 7. The control waveforms were generated with a M531 arbitrary waveform generator from ETC.

Figure 7. Reflectometer prototype used in VKI experiments

The output from the reflectometer was connected to the input channel of a LeCroy Digital Storage Oscilloscope, with 100,000 samples memory size and set to a sampling rate of 10 million samples per second. Several experiments were conducted, corresponding to different Plasmatron operating conditions and different acquisition modes (single-shot vs. sequenced). In single-shot experiments, the signal from the output of the reflectometer was sampled continuously for up to 100 sweeps, or 10 milliseconds. In sequenced experiments, only a fraction of each sweep is

recorded (typically 10 μs, starting at a preset time after the start of the sweep). This allows data to be recorded for longer periods (typically 100 milliseconds).

Data analysis is currently underway. Preliminary results include the detection of reflections from plasma, the existence of frequency dependent features which indicate the existence of measurable plasma profiles in these experiments, and the existence of time dependent features that signal the presence of plasma oscillations. Figure 8 represents the average spectrogram of data resulting from a single-shot experiment, lasting over 100 consecutive sweeps. The horizontal axis represents time from the start of the sweep, with plasma frequency increasing from $t = 0$ to $t = 100$ μs. The vertical axis represents beat frequency f_b, and is proportional to total propagation delay τ. Qualitative examination of this spectrogram indicates that the plasma density increases radially towards the axis of the jet.

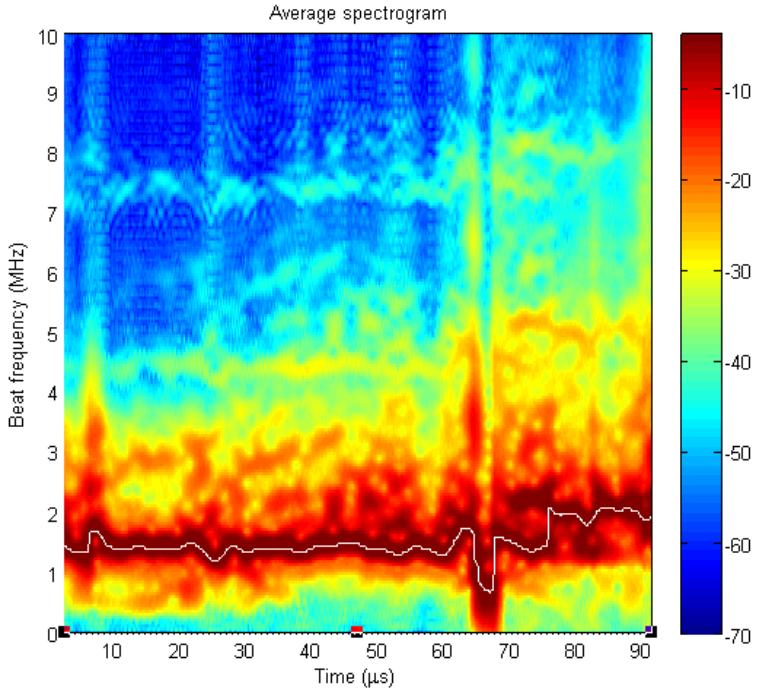

Figure 8. Average spectrogram resulting from 100 consecutive sweeps

Ongoing work includes integrating the various parts of the diagnostic into a single prototype, solving outstanding hardware issues (such as achieving a higher repeatability of the source signals and synchronizing the acquisition with the control waveform), validating the data processing, and performing calibration tests.

V. Conclusion

Plasma reflectometry is under development as an atmospheric reentry diagnostic and is undergoing testing at the VKI plasmatron in Belgium. The diagnostic is a single frequency FMCW broad band swept system. Preliminary testing has indicated the system is operating as anticipated. Frequency dependent reflection of electromagnetic waves from plasma is observed from which it is possible to obtain a spectrogram. The spectrogram is the basic data output from such a system. The plasma profile itself is subsequently obtained from an Abel inversion on the spectrogram. Since the plasma plume in a HET has the same qualitative distribution as the plasmatron, plasma reflectometry is a useful diagnostic for HET ground facilities as well as flight scenarios. Due to the different plasma levels involved in reentry and HET applications, the appropriate frequency range, sweep time, and range gating should be optimized to meet HET requirements.

Acknowledgments

Funding from ESA under contract C21352 for reflectometer development is gratefully acknowledged. Kind hospitality on behalf of Prof. O. Chazot as well access to the Plasmatron facility and technical support at VKI is also acknowledged.

References

[1]C. B. Heald and M. A. Wharton, *Plasma Diagnostics with Microwaves* (Wiley, New York, 1969).
[2]V. L. Ginzburg, *The Propagation of Electromagnetic Waves in Plasmas (*Pergamon, Oxford, 1970).
[3]J. Sheffield, *Plasma Scattering of Electromagnetic Radiation (*Academic, New York, 1975).
[4]H. Soltwick, Trans. Fus. Technol. **25**, 304, 1994.
[5]G. A. Birkner, H. K. Hallock, and H. Ling, Rev. Sci. Instrum. **61**, 2978 (1990).
[6]J. Dickens, Ph.D. thesis, Texas Tech University, 1995.
[7]J. Dickens, M. Kristiansen, and E. O"Hair, IEPC, Moscow, Russia, 1995, pp. 95–171.
[8]J. Dickens *et al.*, 31st AIAA/ASME/SAE/ASEE Joint Propulsion Conference and Exhibit, San Diego, CA, 1995, AIAA 95-2929.
[9]S. Ohler, B. Gilchrist, and A. Gallimore, 30th AIAA/ASMA/SAE/ASEE Joint Propulsion Conference, Indianapolis, IN, 1994, AIAA 94-3297.
[10]S. Ohler, B. Gilchrist, and A. Gallimore, 31st AIAA/ASME/SAE/ASEE Joint Propulsion Conference and Exhibit, San Diego, CA, July 1995, AIAA 95-2931.
[11]M. Born and E. Wolf, *Principles of Optics*. New York: Pergamon, 1964, p. 121.
[12]S. W. Janson, 25th Plasmadynamics and Lasers Conference, Colorado Springs, CO, 1994, AIAA 94-2424.
[13]R. R. Hofer, P. Y. Peterson, A. D. Gallimore, *Characterizing vacuum facility backpressure effects on the performance of a Hall thruster*, Proceedings of the 27th International Electric Propulsion Conference, Pasadena, CA, paper **01-045** (2001).
[14]S. G. Ohler, B. E. Gilchrist, and A. D. Gallimore, IEEE Trans. Plasma Sci. **23**, 428 (1995).
[15]L. Overzet and M. Hopkins, J. Appl. Phys. **74**, 4323 (1993).
[16]O. Duchemin, P. Dumazert, D. Estublier, F. Darnon, N. Cornu, *Stretching the operational envelope of the PPSX000 plasma thruster*, Proceedings of the 40th Joint Propulsion Conference and Exhibit, Ft. Lauderdale, FL, *AIAA paper* **04-3605** (2004).
[17]G. Neumann *et al.*, Rev. Sci. Instrum. **64**, 19 (1993).
[18]Bottin, B. et al. The VKI Plasmatron characteristics and performance. *RTO EN 8,* 1999.
[19]Jan Thoemel, Department of Aeronautics and Aerospace, von Kárman Institute, Belgium (private communication)
[20]B.E. Beal, A.D. Gallimore, and W.A. Hargus, Plasma Properties Downstream of a low power Hall thrusters, POP, 12, 123503 (2005).
[21]J. P. Boeuf and L. Garrigues, J. Appl. Phys. **84**, 3541 _1998
[22]E. Y. Choueri, Phys. Plasmas **8**, 1411 (2001)
[23]Y. Esipchuck, A. Morozov, G. Tilinin, and A. Trofimov, Sov. Phys. Tech. Phys. **18**, 928 (1974)
[24]A. A. Litvak, T. Raitses, and N. J. Fisch, Phys. Plasmas **11**, 1701 (2004).
[25]A. Lazurenko, V. Vial, M. Prioul, and A. Bouchoule, Phys. Plasmas **12**, 013501 (2005).
[26]J.-C. Adam, A. Héron, and G. Laval, Phys. Plasmas **11**, 295 (2004).